NANO LETTERS

2001
Vol. 1, No. 8
429−433

Synthesis and Photoluminescence of Nanocrystalline ZnS:Mn^{2+}

J. F. Suyver,* S. F. Wuister, J. J. Kelly, and A. Meijerink

Debye Institute, Physics and Chemistry of Condensed Matter, Utrecht University, P.O. Box 80.000, 3508 TA Utrecht, The Netherlands

Received May 14, 2001; *Revised Manuscript Received July 16, 2001*

ABSTRACT

The influence of the synthesis conditions on the properties of nanocrystalline ZnS:Mn^{2+} is discussed. Different Mn^{2+} precursors and different ratios of the precursor concentrations [S^{2-}]/[Zn^{2+}] were used. The type of Mn^{2+} precursor does not have an effect on the luminescence properties in the synthesis method described. On going from an excess of [Zn^{2+}] to an excess of [S^{2-}] during the synthesis, the particle diameter increases from 3.7 to 5.1 nm, which is reflected by a change in the luminescence properties. Photoluminescence measurements also showed the absence of the ZnS defect luminescence around 450 nm when an excess [S^{2-}] is used during the synthesis. This effect is explained by the filling of sulfur vacancies. The ZnS luminescence is quenched with an activation energy of 62 meV, which is assigned to the detrapping of a bound hole from such a vacancy.

Over the past few years, considerable interest in the novel optical and electrical properties of doped semiconductor nanocrystals (NC) has emerged.[1−5] These structures are interesting from a physical and chemical point of view mainly because several of their properties are very different from those of bulk materials.[3] Especially, the significant size-dependent shift in the band gap has attracted much attention. This so-called quantum-size effect allows one to tune the emission and excitation wavelengths of a nanocrystal by tuning the crystal radius *r*. A quite good first-order approximation to calculate the energy of the band gap is given by the Brus equation.[1] In the case of zinc blende ZnS, the bulk values of all the materials parameters are known.[6] For nanocrystalline ZnS this results in a relation between the particle radius *r*, in nanometers, and the band gap *E*, in electronvolts, as follows:

$$r(E) = \frac{0.32 - 2.9\sqrt{E - 3.49}}{2(3.50 - E)} \qquad (1)$$

Manganese-doped materials represent a class of phosphors that have already found their way into many applications. The $^4T_1 \rightarrow {}^6A_1$ transition within the $3d^5$ configuration of the divalent manganese ion (Mn^{2+}) has been studied extensively and its orange-yellow luminescence in ZnS is well documented. This luminescence was also observed in nanocrystalline ZnS:Mn^{2+} [7,8] and applications have already been suggested.[9−11] Different types of Mn^{2+} centers are present in nanocrystalline ZnS:Mn^{2+}.[12,13] The orange luminescence originates from Mn^{2+} ions on Zn^{2+} sites, where the Mn^{2+} is tetrahedrally coordinated by S^{2-}.

Previous workers have always used equal concentrations of Zn^{2+} and S^{2-} precursors in the synthesis of these ZnS:Mn^{2+} nanocrystals. This letter will focus on the effect of the synthesis conditions on several properties of these nanocrystals. Two different Mn^{2+} precursors were used and the influence of the ratio of [Zn^{2+}] to [S^{2-}] was investigated. The experimental comparison will include measurements of the diameter, reflectivity, temperature-dependent photoluminescence (PL) emission and excitation as well as luminescence lifetimes. From these results, new insights into the ZnS-related luminescence are obtained and a qualitative explanation will be provided for the phenomena observed.

The inorganic synthesis used to prepare ZnS:Mn^{2+} nanocrystals is similar to that described in the literature.[14] All steps of the synthesis were performed at room temperature and under ambient conditions. The final volume of solution that resulted from the synthesis was kept constant at 100 mL. To ensure that the nanocrystals would not grow into bulk crystals when they agglomerate, a capping polymer was used. For each synthesis *x* mL of a 0.85 M $Na_2S{\cdot}9H_2O$ solution was used. First, 10.2 g of $Na(PO_3)_n$ was dissolved in (80 − *x*) mL of ultrapure water ($R \sim 16$ MΩ). While the solution was stirred, 10 mL of a 1 M $Zn(CH_3COO)_2{\cdot}2H_2O$ solution was added. Next, the Mn^{2+} precursor was added: 10 mL of either a 0.1 M $MnCl_2{\cdot}4H_2O$ solution or a 0.1 M $Mn(CH_3COO)_2{\cdot}4H_2O$ solution. Finally, *x* mL of the sulfide solution was added to the mixture. Immediately after the sulfide solution was added, an opaque white suspension was formed. After centrifuging and washing the particles twice

* Corresponding author. Tel.: +31-30-2532214. Fax: +31-30-2532403. E-mail: j.f.suyver@phys.uu.nl.

10.1021/nl015551h CCC: $20.00
Published on Web 08/08/2001

with distilled water and once with ethanol, the particles were left to dry in a vacuum desiccator for at least 15 h. This resulted in a fine powder with a white or yellowish color, depending on the amount of S^{2-} used in the synthesis (an excess of S^{2-} gives a yellowish product).

To determine the average particle diameter, X-ray powder diffraction spectra were measured with a Philips PW 1729 X-ray generator using Cu Kα radiation at a wavelength of 1.542 Å. The X-ray diffraction (XRD) spectrum showed broad peaks at positions that are in good agreement with the zinc blende modification of ZnS. The broadening of the XRD lines is attributed to the nanocrystalline nature of the samples and was used to calculate the diameter d of the nanocrystals by means of the Debye−Scherrer equation.[15] It is known that the Debye−Scherrer equation gives reasonably accurate values for the particle diameter, comparable to values obtained via high-resolution TEM measurements.[14]

The reflectivity of the samples was measured using a Perkin-Elmer Lambda 16 UV/vis spectrometer. Emission and excitation spectra were recorded with a SPEX Fluorolog spectrofluorometer, model F2002, equipped with two monochromators (double-grating, 0.22 m, SPEX 1680) and a 450 W xenon lamp as the excitation source. All PL spectra were corrected for the spectral response of the emission monochromator and the PM tube. Temperature-dependent emission spectra were recorded using a liquid helium flow-cryostat equipped with a sample heater to stabilize the temperature between 4 K and room temperature. The chemical composition of the samples was determined using a Perkin-Elmer Optima-3000 inductively coupled plasma (ICP) spectrometer.

Since the goal of this letter is to study the influence of the synthesis on the properties of these nanocrystals, all data in this letter will show the precursor ratio $[Zn^{2+}]$ to $[S^{2-}]$ instead of the actual amounts of Zn^{2+} and S^{2-} present in the samples. However, these concentrations have been measured using ICP. From these measurements it was concluded that an excess of either Zn^{2+} or S^{2-} precursor during the synthesis indeed resulted in an excess of Zn^{2+} and S^{2-} present in the samples. When a precursor ratio of $[Zn^{2+}]/[S^{2-}] = 2.3$ was used, the actual ratio of Zn^{2+} or S^{2-} present in the samples was found to be 1.3, while a precursor ratio of 0.5 resulted in an actual ratio of 0.9.

Figure 1 shows the diameter of the nanocrystals determined from the XRD measurements. An identical trend is visible both for the nanocrystals made using $MnCl_2$ and $Mn(CH_3COO)_2$ as a Mn^{2+} precursor. When an excess of S^{2-} instead of a stoichiometric concentration is used in the synthesis, the average nanocrystal diameter is significantly larger than when an excess of Zn^{2+} is used. From the data presented in Figure 1, it is seen that an excess of S^{2-} results in nanocrystals with a diameter of 5.1 ± 0.3 nm while an excess of Zn^{2+} results in nanocrystals with a diameter of 3.7 ± 0.2 nm. Thus, excess $[S^{2-}]$ gives an increase of the particle diameter of $\Delta\langle d_x\rangle = 1.3 \pm 0.4$ nm according to XRD powder measurements. It is important to note that in this analysis the polydispersity was not taken into account. The polydispersity has been measured to be not larger than

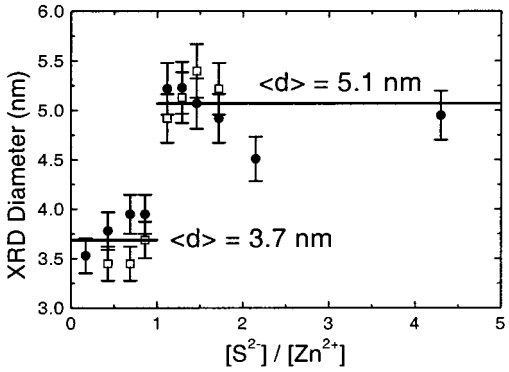

Figure 1. Size of the nanocrystals as derived from XRD and the Debye−Scherrer equation. Samples were made using either $MnCl_2$ (●) or $Mn(CH_3COO)_2$ (□) as the Mn^{2+} precursor.

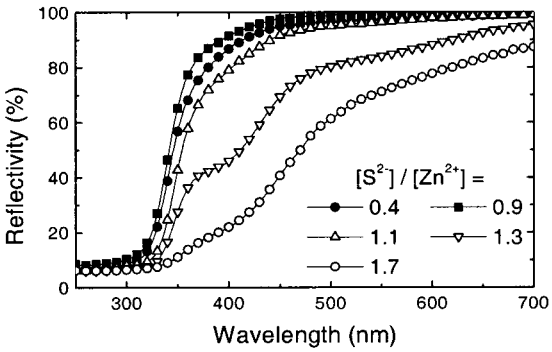

Figure 2. Reflectivity measurements of the ZnS:Mn^{2+} nanocrystals. Samples were made using either $MnCl_2$ (closed symbols) or $Mn(CH_3COO)_2$ (open symbols) as the Mn^{2+} precursor. The $[S^{2-}]/[Zn^{2+}]$ precursor ratios used for the different samples are indicated.

15% based on transmission elecron microscope measurements and no dependence on the $[Zn^{2+}]/[S^{2-}]$ ratio was observed.[16]

Figure 2 shows reflectivity measurements on the samples described. The data presented in this figure corroborate the conclusion made on the basis of Figure 1: there is a shift in the onset of absorption to lower energy on going from an excess of $[Zn^{2+}]$ to an excess of $[S^{2-}]$. This shift in the onset of absorption is due to the change in the nanocrystal band gap. The particle size was calculated from the absorption spectrum, using eq 1. The band gap energy is defined as the energy for which the reflectivity has dropped to 50% of the difference between the transmission in the plateau before the ZnS absorption onset and the transmission at 280 nm. An increase in the average particle size based on the reflectivity measurements of $\Delta\langle d_r\rangle = 0.9 \pm 0.2$ nm was found. This agrees with the $\Delta\langle d_x\rangle$ calculated from the XRD measurements.

The second feature that is clearly visible is the decrease in reflectivity when an excess of $[S^{2-}]$ is used. This trend is also visible to the naked eye: the samples acquire a yellowish color. This color is attributed to elementary sulfur probably on the surface of the nanocrystals. Also, a small fraction of MnS may be formed (dark brown and nonluminescent). No evidence for the formation of colloidal sulfur is found from the XRD spectra. The strong absorption in the visible part of the spectrum for samples made with an excess of S^{2-}

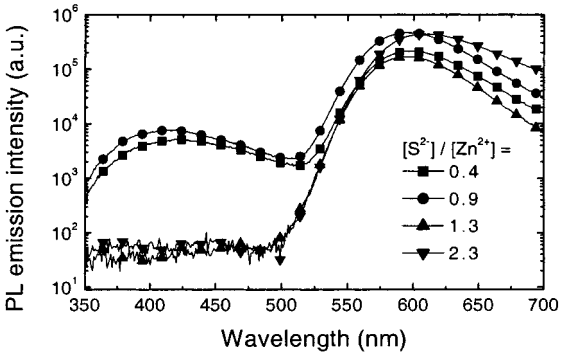

Figure 3. Emission spectra for the samples made with $MnCl_2$ as the Mn^{2+} precursor and different $[S^{2-}]/[Zn^{2+}]$ ratios. All spectra were recorded at room temperature for 300 nm excitation. Note the logatithmic intensity scale.

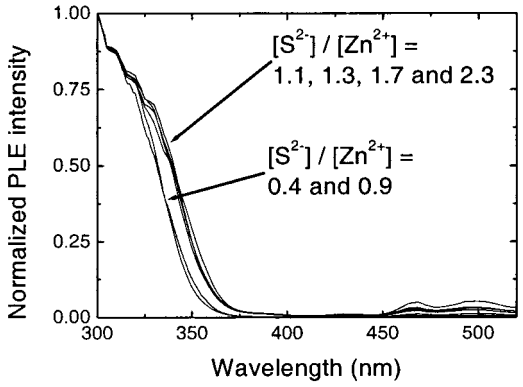

Figure 4. Excitation spectra of the Mn^{2+} emission ($\lambda = 590$ nm) at room temperature for the samples made with different $[S^{2-}]/[Zn^{2+}]$ precursor ratios. The Mn^{2+} precursor was $MnCl_2$ and all excitation spectra were normalized at 300 nm.

makes it difficult to clearly observe the shift in band gap as a function of the $[S^{2-}]/[Zn^{2+}]$ ratio. The excitation spectra, discussed below in Figure 4, provide clear evidence for this effect.

Figure 3 shows PL emission spectra for samples made using $MnCl_2$ as the Mn^{2+} precursor. Relative intensities can be compared. The spectra show two broad peaks. The first one at ~420 nm is also observed for undoped ZnS and is attributed to defect-related emission of the ZnS. This emission was reported in the literature[17] to be a ZnS-related luminescence with a short lifetime. The well-known ZnS-related luminescence of zinc vacancies (at ~480 nm) is not observed in these nanocrystals, indicating that this emission is completely quenched by energy transfer to the Mn^{2+}. Because of the relatively long lifetime of the ~480 nm luminescence, radiative decay cannot compete with energy transfer to Mn^{2+}. The short lifetime of the ~420 nm luminescence allows it to compete with this energy transfer and is still observed, albeit weaker than in undoped ZnS samples. The nature of this ZnS-related luminescence will be discussed below. The peak at ~590 nm corresponds to the $^4T_1 \rightarrow {}^6A_1$ transition in Mn^{2+}. The spectra of the samples made from $Mn(CH_3COO)_2$ are comparable and show very similar results.

It is clear that increasing the S^{2-} concentration beyond the stoichiometric ratio leads to a decrease of about 2 orders of magnitude in the ZnS-related luminescence, while there is no significant effect on the Mn^{2+}-related luminescence. It is interesting to note that a similar trend was observed for large (~1 μm) ZnS:Mn^{2+} colloidal systems.[18] However, for these large particles the effect on the ZnS-related luminescence was not as pronounced, which is probably due to the much smaller surface-to-volume ratio of these colloids. The change in emission spectrum of the nanocrystals did not change the overall quantum efficiency significantly. This is due to the fact that the dominant (Mn^{2+}-related) luminescence is not strongly affected.

Photoluminescence excitation measurements were also performed by exciting the doped nanocrystals in the wavelength region 300−520 nm while monitoring the Mn^{2+} emission (~590 nm) or the ZnS emission (~420 nm). Figure 4 shows the excitation spectrum of the Mn^{2+}-related PL for several $[S^{2-}]/[Zn^{2+}]$ precursor ratios. A clear maximum in the Mn^{2+}-related emission intensities was observed at an excitation wavelength of roughly 330 nm (particle size dependent), which indicates that the Mn^{2+} excitation takes place via energy transfer from the ZnS host lattice. In these excitation spectra, a clear (86 meV) blue shift is observed when going from a synthesis with excess S^{2-} (ratios 1.1, 1.3, 1.7, and 2.3) to a S^{2-} deficient synthesis (ratios 0.4 and 0.9). This discrete shift around a $[S^{2-}]/[Zn^{2+}]$ ratio of 1 is in good agreement with the increase in particle diameter, as was observed in both XRD and reflection measurements (see Figures 1 and 2).

The observed changes in particle diameter and luminescence properties can result from two different effects. It must be noted that a 0.85 M solution of Na_2S in water is very alkaline (pH = 13.5). Therefore, the observed changes could be due to either the large change in pH during the synthesis, or to the higher S^{2-} concentration. To verify that the observed changes are not due to the pH, the synthesis was performed by changing the pH of the solution before the S^{2-} precursor was added by means of a 1 M NaOH solution. During these syntheses, the ratio of $[Zn^{2+}]$ to $[S^{2-}]$ precursor was kept at the stoichiometric value.

Figure 5 shows photoluminescence emission spectra for ZnS:Mn^{2+} nanocrystals prepared at several pH values, where 5.4 is the natural pH of the solution for the synthesis method used. Acidic conditions are also shown for comparison. It is clear that even for addition of 50 mL of NaOH (pH_{end} = 8.1) before addition of the S^{2-} precursor, no change in the ZnS-related luminescence was observed. No trend in particle size was found as a result of pH variation. The quenching of the ZnS-related PL when the synthesis is performed in an acidic environment could be due to surface dissolution of the ZnS nanocrystals. This dissolution can introduce quenching sites at the surface of the nanocrystal. Since one of the charge carriers involved in the ZnS-related luminescence is delocalized, the presence of surface quenching sites can result in a decrease of the photoluminescence quantum efficiency.

Since the pH of the Na_2S solution cannot explain the trends observed in Figures 1−4, it must be concluded that these

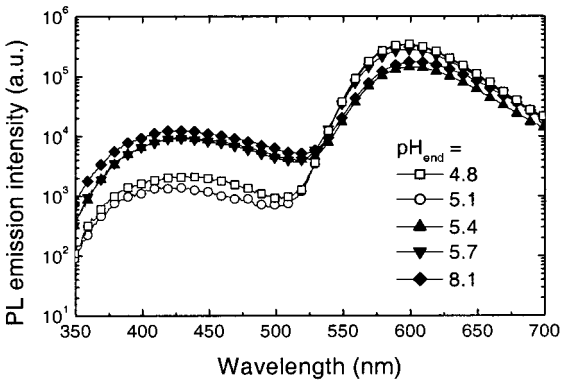

Figure 5. Emission spectra for the ZnS:Mn^{2+} samples made at different pH levels. All spectra were recorded at room temperature for 300 nm excitation. Note the logatithmic intensity scale.

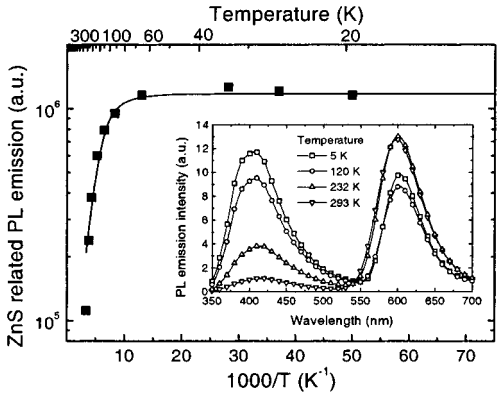

Figure 6. Temperature-dependent photoluminescence emission measurements for a $[Zn^{2+}] = [S^{2-}]$ sample. Excitation was at 300 nm. The drawn line is a fit using eq 2. Inset: Temperature dependence of the ZnS:Mn^{2+} photoluminescence emission spectrum.

are due to the $[S^{2-}]$ present during the synthesis. For ZnO nanocrystals it is known that the ZnO-related luminescence is due to oxygen vacancies ($V_O^{\bullet}$ according to the Kröger−Vink notation for identifying defects[19]) in the crystal[20] and that excess O^{2-} during the synthesis reduces the concentration of these centers and therefore quenches the ZnO PL. It seems reasonable to assume a similar process for ZnS: the $V_S^{\bullet}$ centers are involved in the ZnS defect emission. In the presence of excess S^{2-}, the concentration of $V_S^{\bullet}$ centers will be lower. This does not influence the total QE because the Mn^{2+}-related photoluminescence is the dominant feature in the emission spectrum.

Temperature-dependent PL measurements for a sample made from a solution with equal concentrations of Zn^{2+} and $S^{2-}$are shown in the inset of Figure 6. It is clear from this inset that for lower temperatures, the ZnS-related PL increases in intensity while the Mn^{2+}-related PL decreases. Figure 6 shows the temperature quenching of the ZnS-related luminescence. Fitting an Arrhenius function (continuous line in Figure 6)

$$I(T) = \frac{I_0}{1 + A\exp\left(-\frac{\Delta E}{k_B T}\right)} \qquad (2)$$

gives an activation energy of $\Delta E = 62 \pm 8$ meV.

This temperature dependence of the luminescence intensities indicates that there is a thermally activated energy transfer process with a 62 meV activation energy. To explain the process behind this temperature behavior, it is important to understand the excitation mechanism of both the self-activated (defect) emission and the Mn^{2+} emission. In the literature various mechanisms have been proposed. In the recent literature on the luminescence of nanocrystalline ZnS:Mn^{2+}, it is often suggested that first an electron is captured by Mn^{2+}. However, in the literature on the luminescence of bulk ZnS:Mn^{2+} very careful high-resolution measurements have been reported, which indicate that the Mn^{2+} center is attractive for holes.[21,22] In view of the known oxidation states of manganese (2+, 3+, 4+, and 7+ are well-known, 1+ is not stable) it seems more likely that Mn^{2+} is hole attractive.

On the basis of the measurements, several possible excitation mechanisms for the Mn^{2+} were suggested (see Figure 8 in ref 22). In one mechanism the Mn^{2+} ion first traps a hole and the subsequent recombination with an electron results in Mn^{2+} in the excited state. Alternatively, an exciton may be bound to Mn^{2+} and recombination of the bound exciton promotes the Mn^{2+} to the excited state. Both mechanisms may be active in bulk ZnS:Mn^{2+} and nanocrystalline ZnS:Mn^{2+}.

The excitation of the ZnS:Mn^{2+} nanocrystals starts with the creation of an electron−hole pair. Recombination of the electron−hole pairs can occur via different routes, resulting in nonradiative relaxation, Mn^{2+} emission, or defect-related emission. Nonradiative relaxation will occur at certain defect states or surface states. For efficiently luminescing materials, this process is undesired. In the model for the defect-related emission presented above, first trapping of holes occurs at sulfur vacancies ($V_S^{\bullet}$ according to the Kröger−Vink notation for identifying defects[19]), resulting in a $V_S^{\bullet\bullet}$ state. Subsequent recombination with a (shallowly trapped) electron gives rise to the violet emission:

$$(1) \quad V_S^{\bullet} + h^{+}(VB) \leftrightarrow V_S^{\bullet\bullet}$$

$$(2) \quad V_S^{\bullet\bullet} + e^{-} \rightarrow V_S^{\bullet} + h\nu_1$$

The quenching of the defect-related emission can be understood if the first step is reversible with a back-transfer energy of 62 meV. The emission from Mn^{2+} can be excited either directly by recombination of a bound exciton at Mn^{2+} or via trapping of the hole by Mn^{2+}.[21,22] Subsequent recombination with shallowly trapped electron results in Mn^{2+} in an excited state and is followed by the well-known orange Mn^{2+} emission:

$$(1) \quad Mn^{2+} + h^{+}(VB) \rightarrow Mn^{3+}$$

$$(2) \quad Mn^{3+} + e^{-} \rightarrow (Mn^{2+})^{*}$$

$$(3) \quad (Mn^{2+})^{*} \rightarrow Mn^{2+} + h\nu_2$$

The thermally activated quenching of the defect emission and the accompanying increase in the Mn^{2+} emission can now be understood: at elevated temperatures the holes are detrapped from the $V_S^{\bullet\bullet}$ levels, and part of the holes that are released may now be retrapped by Mn^{2+}. After a subsequent recombination with an electron, Mn^{2+} in excited state is formed, resulting in Mn^{2+} emission. This can explain the increase of the Mn^{2+} in the temperature regime where the violet defect-related emission quenches.

In conclusion, this letter shows that by using an excess of sulfide for the synthesis of nanocrystalline ZnS:Mn^{2+}, the particle diameter is increased by about 1 nm, while the defect-related luminescence from ZnS is no longer observed. The Mn^{2+} luminescence is not affected. These results and the temperature dependence of the defect and Mn^{2+} emission are explained by a model in which sulfur vacancies are involved in the defect luminescence.

Acknowledgment. This work is part of the Research Program of the Priority Program for new Materials (PPM) and was made possible by financial support from the Dutch association for scientific research (NWO).

References

(1) Brus, L. *J. Phys. Chem.* **1986**, *90*, 2555.
(2) Wang, Y.; Herron, N. *J. Phys. Chem.* **1991**, *95*, 525.
(3) Alivisatos, A. P. *J. Phys. Chem.* **1996**, *100*, 13226.
(4) Norris, D. J.; Yao, N.; Charnock, F. T.; Kennedy, T. A. *Nano Lett.* **2001**, *1*, 3.
(5) Kane, R. S.; Cohen, R. E.; Silbey, R. *Chem. Mater.* **1999**, *11*, 90.
(6) Lide, D. R. *Handbook of Chemistry and Physics*, 74th ed.; CRC Press: Boca Raton, FL, 1994.
(7) Bhargava, R. N.; Gallagher, D.; Hong, X.; Nurmikko, A. *Phys. Rev. Lett.* **1994**, *72*, 416.
(8) Sooklal, K.; Cullum, B. S.; Angel, S. M.; Murphy, C. J. *J. Phys. Chem.* **1996**, *100*, 4551.
(9) Xu, C. N.; Watanabe, T.; Akiyama, M.; Zheng, X. G. *Appl. Phys. Lett.* **1999**, *74*, 1236.
(10) Bhargava, R. *J. Lumin.* **1996**, *70*, 85.
(11) Suyver, J. F.; Bakker, R.; Meijerink, A.; Kelly, J. J. *Phys. Stat. Sol. A* **2001**, *224*, 307.
(12) Borse, P. H.; Srinivas, D.; Shinde, R. F.; Date, S. K.; Vogel, W.; Kulkarni, S. K. *Phys. Rev. B* **1999**, *60*, 8659.
(13) Soo, Y. L.; Ming, Z. H.; Huang, S. W.; Kao, Y. H.; Bhargava, R. N.; Gallagher, D. *Phys. Rev. B* **1994**, *50*, 7602.
(14) Yu, I.; Isobe, T.; Senna, M. *J. Phys. Chem. Solids* **1996**, *57*, 373.
(15) Cullity, B. D. *Elements of X-ray Diffraction*; Addison-Wesley: Massachusetts, 1978.
(16) A. A. Bol, private communication.
(17) Oda, S.; Kukimoto, H. *J. Lumin.* **1979**, *18/19*, 829.
(18) Becker, W. G.; Bard, A. J. *J. Phys. Chem.* **1983**, *87*, 4888.
(19) Kröger, F. A. *The chemistry of inperfect crystals*; North-Holland Publishing Co.: Amsterdam, 1973.
(20) van Dijken, A.; Meulenkamp, E. A.; Vanmaekelbergh, D.; Meijerink, A. *J. Phys. Chem. B* **2000**, *104*, 1715.
(21) Hoshina, T.; Kawai, H. *Jpn. J. Appl. Phys.* **1980**, *19*, 267.
(22) Jaszczyn-Kopec, P.; Canny, B.; Syfosse, G. *J. Lumin.* **1983**, *28*, 319.

NL015551H